Article:
Al-Sallami, W, Parsaeian, P orcid.org/0000-0001-8393-3540, Dorgham, A et al. (1 more author) (2019) Reactivity of oil-soluble IL with silicon surface at elevated temperature. Lubrication Science, 31 (4). pp. 151-162. ISSN 0954-0075

https://doi.org/10.1002/ls.1456

Reactivity of oil-soluble IL with silicon surface at elevated temperature

Waleed Al-Sallami[1,*], Pourya Parsaeian[1], Abdel Dorgham[1], Anne Neville[1].

[1]School of Mechanical Engineering, University of Leeds, UK

Abstract

The reactivity of an oil-miscible ionic liquid, phosphonium phosphate (PP), and the common anti-wear additive Zinc Dialkyl Dithio Phosphate (ZDDP) with a solid surface at elevated temperature in the absence of any tribological motion is investigated. Understanding the thermal film build up, composition and relative thickness will help in the understanding of lubrication mechanisms once tribological effects are introduced. ATR-FTIR, SEM-EDS and XPS are employed to characterize silicon surfaces before and after the experiments in terms of surface chemistry and surface morphology. The results showed that both additives react with the silicon surface to produce thermal films. However, ZDDP formed a thicker film. PP reacts with the silicon and forms a thermal film but the reaction rate is self-limited such that an increase of time to 24 h does not significantly increase the film thickness.

Keywords: Soluble IL, ZDDP, tribology, additives, ATR-FTIR, SEM-EDS, XPS and formation of thermal film.

1. Introduction

Current tribological research relevant to the automobile sector is predominantly focused on the reduction of both fuel consumption and the emission of harmful gases and products that impact negatively on the environment. Lowering of friction improves the overall fuel efficiency of the system. Lowered friction must be in an environment of managed wear. Managed wear will maintain the life time of the component, meaning longer periods between services. The latest developments in tribology in terms of reducing friction can lead to 14% and 18% reductions in the consumed fuel in heavy machines and passenger automobiles respectively (1, 2). Concurrently, the CO_2 emissions could be reduced by 200 and 290 million tons for heavy duty machines and passenger automobiles respectively (1, 2).

Advances in tribology include the use of next generation lubricants such as Ionic Liquids (ILs) (3-6), effective anti-wear additives (7), advanced coatings (8) and modifications such as surface texturing (9).

In terms of effective anti-wear additives, Zinc Dialkyl Dithio Phosphate (ZDDP) is one of the most common. However, the production of ash when it is decomposed and the emission of harmful gases push researchers to identify alternatives which can provide comparable anti-wear performance (10-12). Therefore, ashless additives are proposed as anti-wear additives instead of ZDDP (13, 14). Soluble ILs are also suggested to be an effective alternative to ZDDP, especially when lubricating light alloys (15).

Ionic Liquids (ILs) have been suggested as effective alternatives due to their high thermal stability, low vapour pressure, high thermal conductivity and their physical properties can be controlled easily by changing their chemistry. Although IL is used as an all-encompassing term it should be recognized that a wide range of properties are displayed by ILs. ILs are salts that are available in the liquid state over a wide range of temperatures. A large bank of literature exists where the tribological performance of ILs has been investigated and the results implied that ILs can provide a significant reduction in wear and friction for various tribopairs (3-6). Nevertheless, the majority of ILs are insoluble in non-polar lubricants and can be employed as lubricants only rather than lubricant additives to non-polar oils (3-6).

In reported literature, a few oil-miscible phosphonium based ILs have been compared with ZDDP. The results showed that oil-miscible ILs offer superior anti-wear performance especially at elevated temperature when both had comparable concentrations (7, 16-18). The reduction of wear is as a result of the chemical reaction between IL or ZDDP and the interacting surfaces which lead to form a tribofilm (19, 20). However, the reason behind the superior anti-wear performance of soluble IL than ZDDP at elevated temperature is still vague.

The reactivity of ILs with solid surfaces at elevated temperature is still not well defined; aspects of the chemical species formed, the rate of formation and the film thickness need to be measured. It is crucial in the understanding of lubrication mechanisms to understand the thermal adsorption behaviour or thermally-activated chemical reactions in the absence of any tribological effect. In contrast to ILs, a large number of previous papers have focused on the lubrication mechanism of ZDDP (21-24). Some have focused on the reactivity of ZDDP with steel or hard coatings at elevated temperatures (25-29) to obtain a full understanding of its lubrication mechanism. The results have shown that ZDDP is capable of interacting with the examined surfaces and forms a thermal film; the thickness of this film is increased with increasing time while the chemistry is strongly influenced by temperature (26, 27). Further, the morphology of the ZDDP thermal film was influenced by both time and temperature.

Increasing one or both of them increases film consistency (30). However, the reactivity of ZDDP with light alloys at elevated temperature is still vague since the previous studies focused on steel, copper and hard coatings (11). In addition, the identification of polyphosphate chain length that resulted from ZDDP tribo/thermal films are studied in (31, 32). They found that polyphosphate chain length can be identified by calculating the ratio of bridging oxygen (BO) to non-bridging oxygen (NBO). The increase of BO to NBO ration results from the decrease of polyphosphate chain length.

In this paper the reactivity of ZDDP and the formation of thermal films on silicon at elevated temperature are studied and compared with PP. This work is presented as a part of a large study and the subsequent paper considers the lubrication performance in a range of engineering contacts. The formation mechanism of thermal film is important as a route to understand the lubrication mechanisms of both additives when lubricating silicon. Formation of thermal film can be resulted from the physically absorbed film, chemically adsorbed film or chemically reacted film (11). Data on ZDDP interactions with silicon is limited; thermal films have not been widely studied. However, relevant to this study is the study of Al-Si tribochemistry since silicon grains were distinct in hyper-eutectic Al-Si alloys. Burkinshaw et al, in (33) demonstrated that the Si reacts tribochemically and it is important for the overall behaviour of the Al-Si tribology in a piston-cylinder assembly. Jimenez et al, in (34) also studied the formation of ZDDP and ZDDP+MoDTC tribofilms on Al-Si alloys. The results showed that both additives have reacted with Al-Si alloy. To the best of the authors' knowledge, this is the first investigation which covers the reactivity of IL with a solid surface at elevated temperature.

2. Materials and Experimental methods

2.1 Materials

N-type Si, from EL-CAT INC., RIDGEFIELD PARK, NJ, USA, is employed in this study. The average roughness (R_a) of the polished side is 0.2 nm as measured using a Bruker Atomic Force Microscope (AFM) in the University of Leeds, UK. The wafer was manually cut into small samples to give dimensions of each sample of 5mm × 5mm. The understanding of the lubrication of silicon is the key part to understand the lubrication of AL-Si alloy (33).

Three lubricants were examined; PAO, PAO+1.08wt% PP and PAO+0.74wt% ZDDP. Fig.1 depicts the chemical structure of all lubricants. PP is purchased from Sigma-Aldrich, ZDDP from Afton Chemicals and PAO from Ineos Oligomers. The selection of these percentages are made to achieve the same phosphorus content of 800 ppm in both blended lubricants. This is

the maximum permitted concentration based on the International Lubricants Standardization and Approval Committee (35). Furthermore, a hot plate with magnetic stirrer are used to blend PP and ZDDP with PAO. Each mixture is heated to 60 ^{o}C and stirred at 200 RPM for 120 minutes. In addition, the PAO+PP blend is sonicated before the experiments.

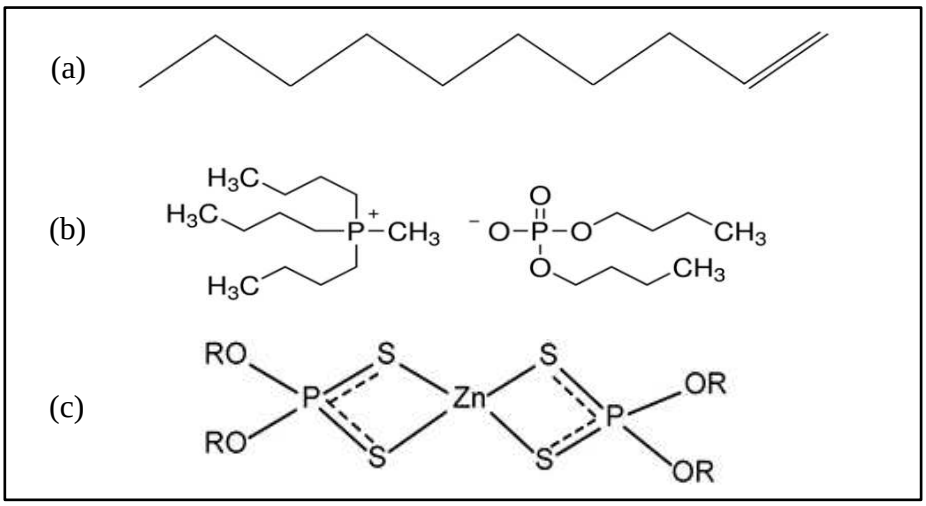

Fig. 1: Lubricants in this study; (a) PAO, (b) PP and (c) ZDDP.

2.2 Thermal film formation procedure

The formation of thermal films is investigated at 150 ^{o}C (2, 6 and 24 hours) and 175 ^{o}C (2, 6 hours). The temperatures are relevant to the working temperatures of an internal combustion engine. A hot plate combined with a feedback control system is used to increase the lubricants' temperature and placed in a well ventilated chamber to ensure that any produced fumes will be exhausted directly. Further, all silicon samples are sonicated in methanol for 10 minutes to clean any residue before starting the experiment. Lastly, the silicon samples are sonicated again in methanol for 3 minutes after each experiment to remove residue.

2.3 Chemical characterization of lubricants and surfaces

2.3.1 Attenuated Total Reflection - Fourier Transform Infra-Red (ATR-FTIR) spectroscopy

The PerkinElmer spectrum 100 FTIR in the University of Leeds is used to probe the nature of any reacted film on the silicon surface. All silicon samples before and after the generation of thermal films were examined. A ZnSe crystal is employed and the detector type is a combination of ATR with spectrum 100. The sampling depth at 45^{o} is about 1.66 µm (36). The signal is recorded in the range between 650 to 4000 cm^{-1} and at least 50 scans are collected with a resolution of 4 cm^{-1} and the number of reflection is 1. After that, the obtained spectra

are analysed based on the strength and wave number of each peak, by matching them with the available data in (37).

2.3.2 Scanning Electron Microscopy – Energy Dispersive Spectroscopy (SEM-EDS)

The Hitachi SEM-EDS in Leeds Electron Microscopy and Spectroscopy (LEMAS) is utilized in this study to investigate thermal film morphology using SEM and surface chemical composition map using EDS. The sampling depth of EDS is about 2-5 µm (38). All samples after the generation of thermal films of both additives were examined. This technique was employed after ATR-FTIR since silicon samples require preparation before measurement including carbon coating to avoid charging (39).

2.3.3 X-ray Photoelectron Spectroscopy (XPS)

XPS is used to reveal surface chemistry since it can detect very thin films; its sampling depth can be lower than 7 nm (40). Five samples are examined; as prepared P-doped silicon substrate and the samples exposed to 150 ^{o}C for 2 hours in either ZDDP or PP and at 175 ^{o}C for 6 hours in either ZDDP or PP. These two conditions were selected for XPS analysis because they represent the lowest and highest examined temperatures.

A Kratos AXIS Nova XPS in the University of Newcastle, UK, is utilized. A monochromatic Al Kα (1486.6 eV) beam is employed and the spot size was 300 µm. Three spots are scanned in each sample to investigate the homogeneity of the formed films. This XPS system also contains an optical microscope which allows users to obtain 700 × 300 micron images and the scanned area can be specified from this image.

In addition, three sweeps are applied to obtain the survey scan (low resolution) and ten sweeps for high resolution regions. The pass energies are 160 eV and 20 eV for survey and high resolution regions respectively. For all samples the survey scan is collected in the range of binding energy between 0 and 1200 eV and based on the obtained results the high resolution regions are specified. However, to avoid the interference between silicon electrons, that resulted from the Plasmon effect, and both phosphorus and sulfur electrons; P2s and S2s are scanned at high resolution instead of the P2p and S2p regions (41).

CasaXPS is employed for curve fitting using the Gaussian-Lorentzian method. The calibration to achieve charge correction is fulfilled based on carbon spectrum (C1s) when it is shifted to 285 eV (42). On the other hand, quantitative analyses are performed using corrected area A0 by dividing the obtained area by the sensitivity factor Sf. This factor can be calculated using

the following equation; Sf = σ. Λ. B. T, when σ is photoionization cross-section and it can be obtained from (43), Λ inelastic mean free path and the calculation method is available in (44), B is the asymmetry parameter and it is obtained from (45) and lastly, T is representing the analyser transmission function.

3. Results

3.1 Surface analysis results

3.2.1 ZDDP thermal film results

Fig. 2 depicts the FTIR results for the silicon surfaces before the generation of ZDDP thermal film. It is clear that silicon surface is clear of any compounds that can be detected by FTIR. Fig. 3 demonstrates the FTIR results of silicon samples after the generation of ZDDP thermal films. The results show that among the five conditions only for 2h 175 ^{o}C, 6h 175 ^{o}C and 24h 150 ^{o}C, were peaks detected and that showed the presence of a thermal film. The peak at 926 cm^{-1} can be assigned to either stretching vibration of P=O (25) or the asymmetric vibration of P-O-P (42). A peak at 1087 cm^{-1} is detected and it can be assigned to the asymmetric vibration of either PO_3 or SO4 (42, 46). The peak at 1125 cm^{-1} can be assigned to either the stretching vibration of P-O-Si (25), asymmetric vibration of PO_3^{-2} (42, 46) or an overlap of both peaks. For the longest period, 24 h, a new weak peak is obtained at 750 cm^{-1} which can be assigned to the symmetric vibration of P-O-P (25). Also, a peak at 1640 cm^{-1} can be assigned to C=C (25).

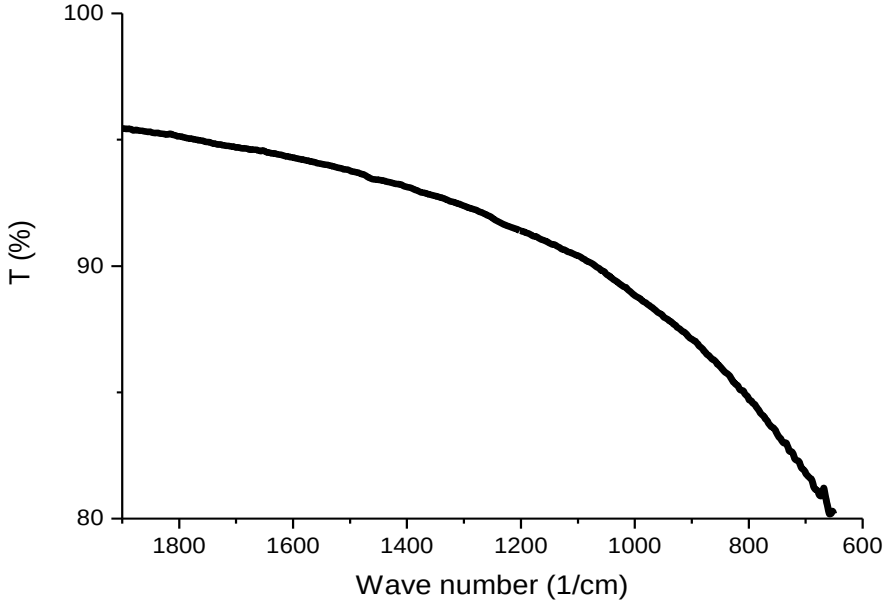

Fig. 2: FTIR results for silicon substrate before the generation of thermal film and after the formation of PP thermal film.

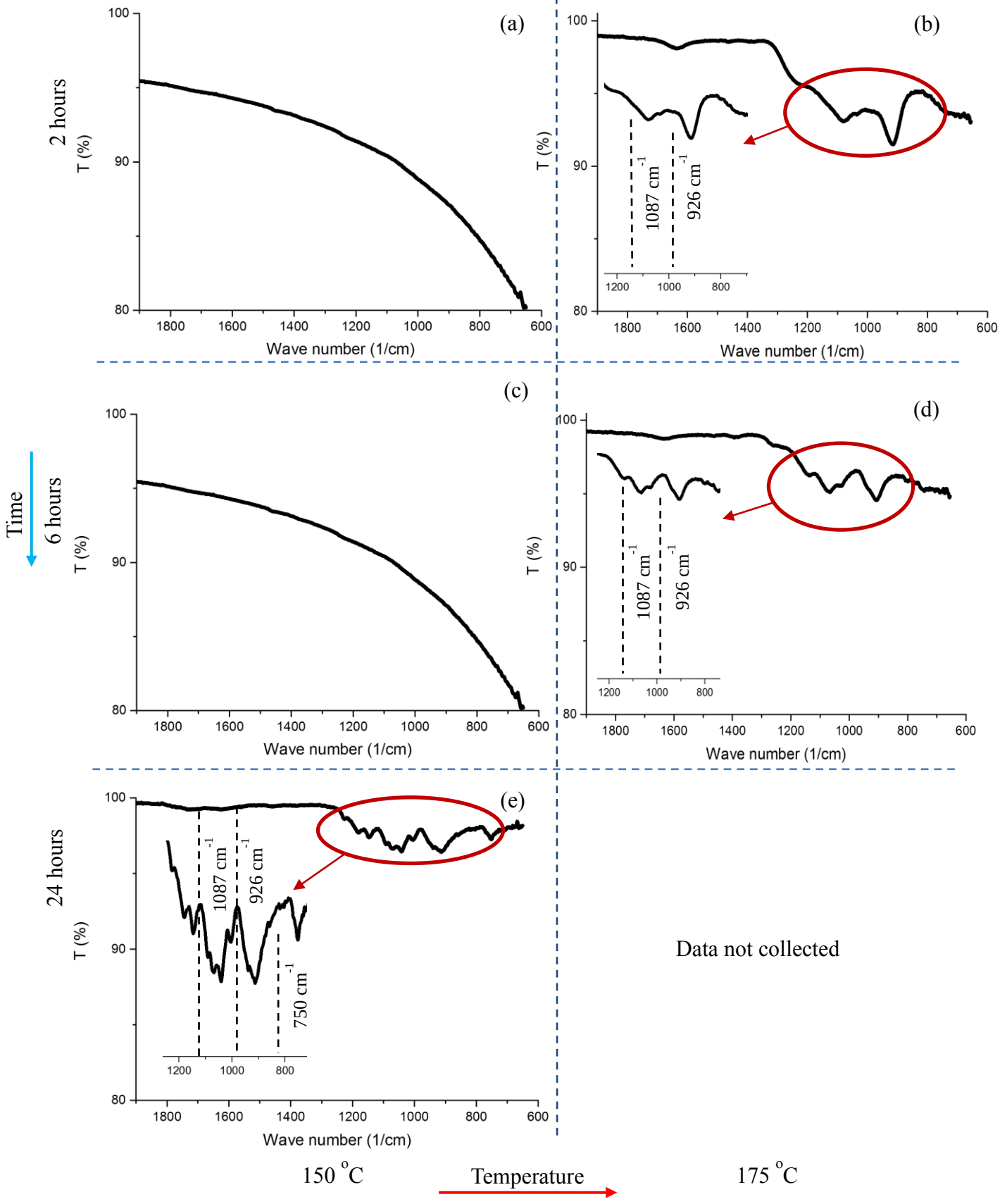

Fig.3: **:** FTIR results for ZDDP thermal film at the following conditions: (a) 150 ºC and 2 hours, (b) 175 ºC and 2 hours, (c) 150 ºC and 6 hours, (d) 175 ºC and 6 hours and (e) 150 ºC and 24 hours.

The surface morphologies of Si before and after the formation of ZDDP thermal film under all applied conditions are demonstrated in the SEM images in Fig. 4. It can be seen clearly that both film thickness and film consistency are increased with the increase of either temperature or time. In addition, the elemental mapping of the created films from EDS analysis showed that all surfaces have the same elements; phosphorus, zinc, carbon, silicon and oxygen. Fig. 5 depicts EDS result of ZDDP thermal film after the longest period at 24h. It can be seen that the presence of silicon significantly decreased when the thermal film is formed. The presence of oxygen, zinc and phosphorus is increased with the formation of thermal film. The presence of carbon is comparable before and after the formation of thermal film.

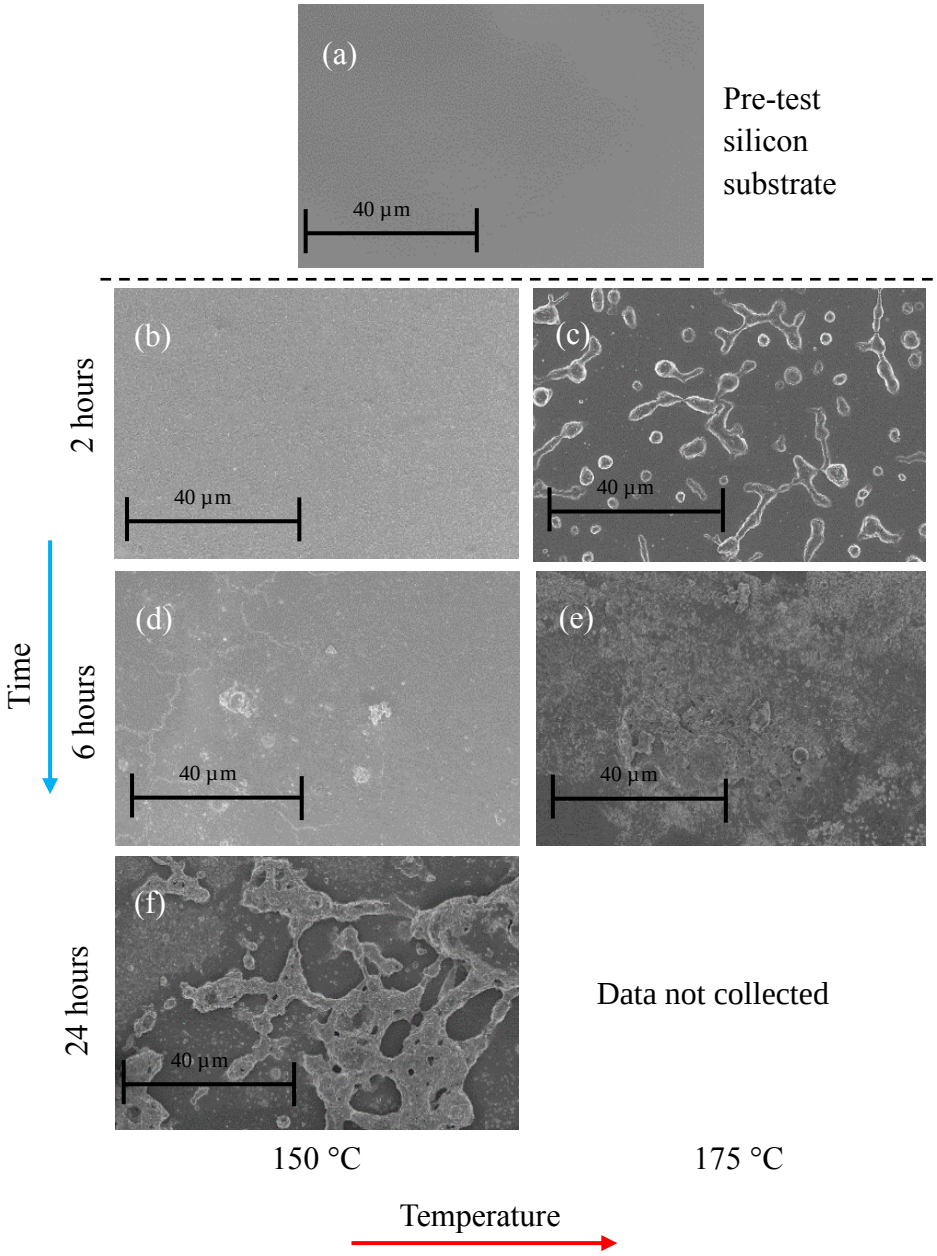

Fig. 4: Surface morphology of (a) Si substrate before test; (b) Si in ZDDP 150 ^{o}C 2h; (c) Si in ZDDP 175 ^{o}C 2h; (d) Si in ZDDP 150 ^{o}C 6h (e) Si in ZDDP 175 ^{o}C 6h and (f) Si in ZDDP 150 ^{o}C 24h.

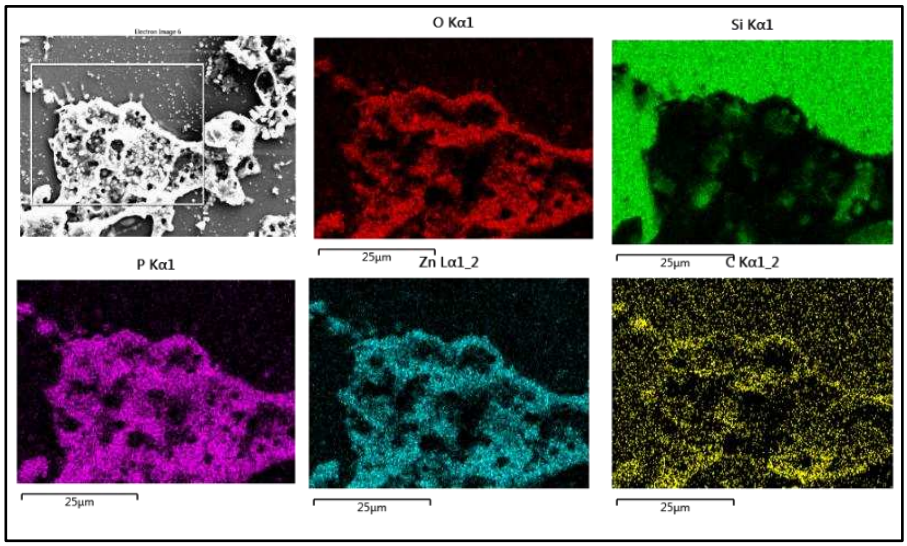

Fig. 5: The EDS result of ZDDP thermal film at 150 ºC and for 24 h.

The results of XPS again confirm the formation of the thermal film when zinc, phosphorus and sulfur are detected. Three spectra are collected; P2s, S2s, Zn2p which are the elements that resulted from the chemical reaction between ZDDP and silicon surface.

Sulfur is detected only at 2h and 150 ºC, see Fig. 6. S2s at 226.6 eV is fitted with one peak and assigned to ZnS (47), which is also confirmed by Zn2p peak. The S2s peak is diminished with the increase of time and temperature which means that sulfur in ZnS is dissociated.

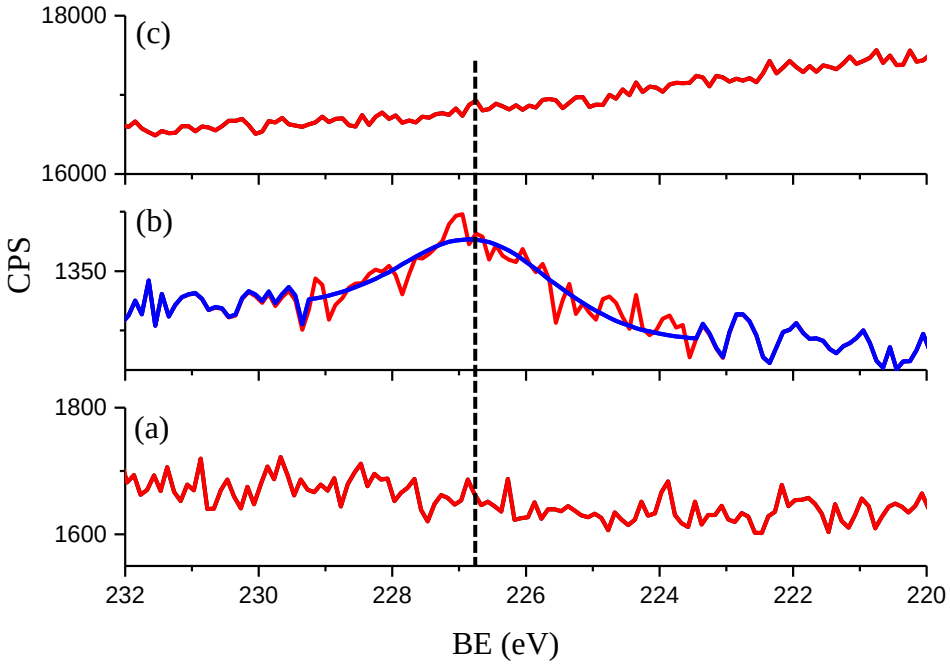

Fig. 6: S2s peak for (a) silicon before experiment, (b) ZDDP thermal film formed at 2h and 150 ºC and (c) ZDDP thermal film formed at 6h and 175 ºC.

Zinc is detected in both conditions; 150 ºC (2 hours) and 175 ºC (6 hours), and Zn2p is scanned as a high resolution region. Fig. 7 presents the Zn2p peaks, fitted into two peaks (Zn2p 3/2 and Zn2p 1/2). At lower temperature the Zn2 p3/2 at 1022 ev is assigned to ZnS (48) which is in agreement with the sulfur assignment. The increase of both time and temperature lead to a shift the peak by 0.6 eV which means that the chemical state has been changed. This shifting is as a result of oxidation of Zn and the new peak is assigned to ZnO (48). The Zn2p of ZnO and ZnS are close to each other (1022 eV and 1022.6 eV) respectively; in this paper the XPS results of Zn and S have been used to suggest that there is a change from ZnS to ZnO.

P2s is also detected at both conditions as shown in Fig. 8. However, phosphorus already exists in the n-type silicon. In order to distinguish between phosphorus created by the thermal film and phosphorus element that exists in the substrate; both the intensity ratio of P2s to Si2s and the binding energy are utilized. The intensity ratio of P2s to Si2s, that existed due to plasmon effect, is 0.5 and the binding energy of P2s is 187.7 eV which is in agreement with (41).

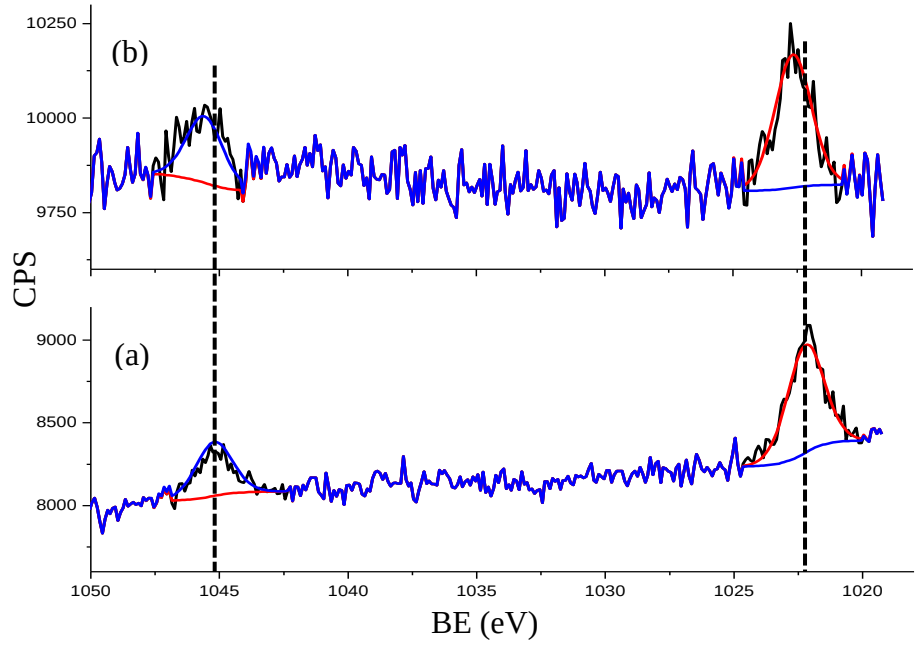

Fig. 7: Zn2p peak for (a) ZDDP thermal film formed at 2h and 150 ºC and (b) ZDDP thermal film formed at 6h and 175 ºC.

After the formation of the thermal film; both the silicon plasmon peak and the phosphorus peak are diminished. Two new peaks are obtained at 188.6 eV and at 191.5 eV. The interpretation of these two peaks is done using information from FTIR results and the available data in (41). The first peak at 188.6 eV can be assigned to phosphate as shown in FTIR results. The second peak at 191.5 eV can be assigned to P-O-Si which is in agreement with (41), FTIR results in the current study and FTIR results in (25).

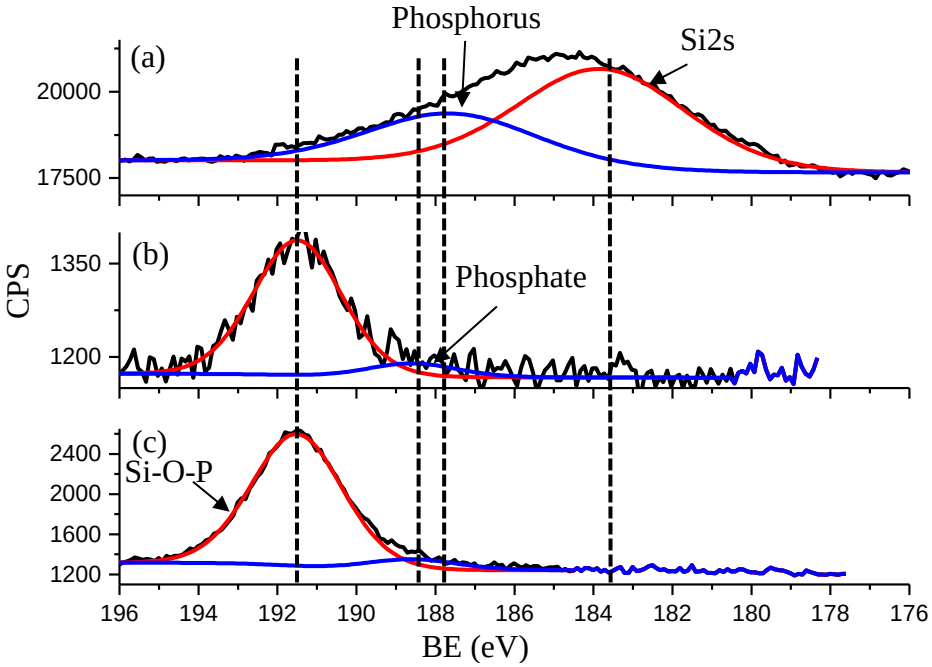

Fig. 8: P2s peak for (a) silicon before experiment, (b) ZDDP thermal film formed at 2h and 150 ºC and (c) ZDDP thermal film formed at 6h and 175 ºC.

Lastly, table 3-1 presents the chemical composition of ZDDP thermal film at two conditions (150 ºC for 2 hours and 175 ºC for 6 hours). The results show a plenty of carbon exists which can be resulted from the traces of both the base lubricant (PAO) and ZDDP. The atomic percentage of phosphorus increases with the increase of time and temperature. This finding is in agreement with SEM-EDS and FTIR results since both confirm that the film thickness increases with time and temperature.

3.2.2 PP thermal film results

Using ATR-FTIR, the thermal film of PP could not be detected under any of the applied conditions (as shown in Fig.2). This means that the created film is not thick enough to be detected by FTIR. The sampling depth of the ZnSe crystal is about 1.66 µm (36). SEM-EDS is used in order to characterize the topography of the silicon surface before test and after the formation of PP thermal films under various circumstances as shown in Figs. 9. and 10.

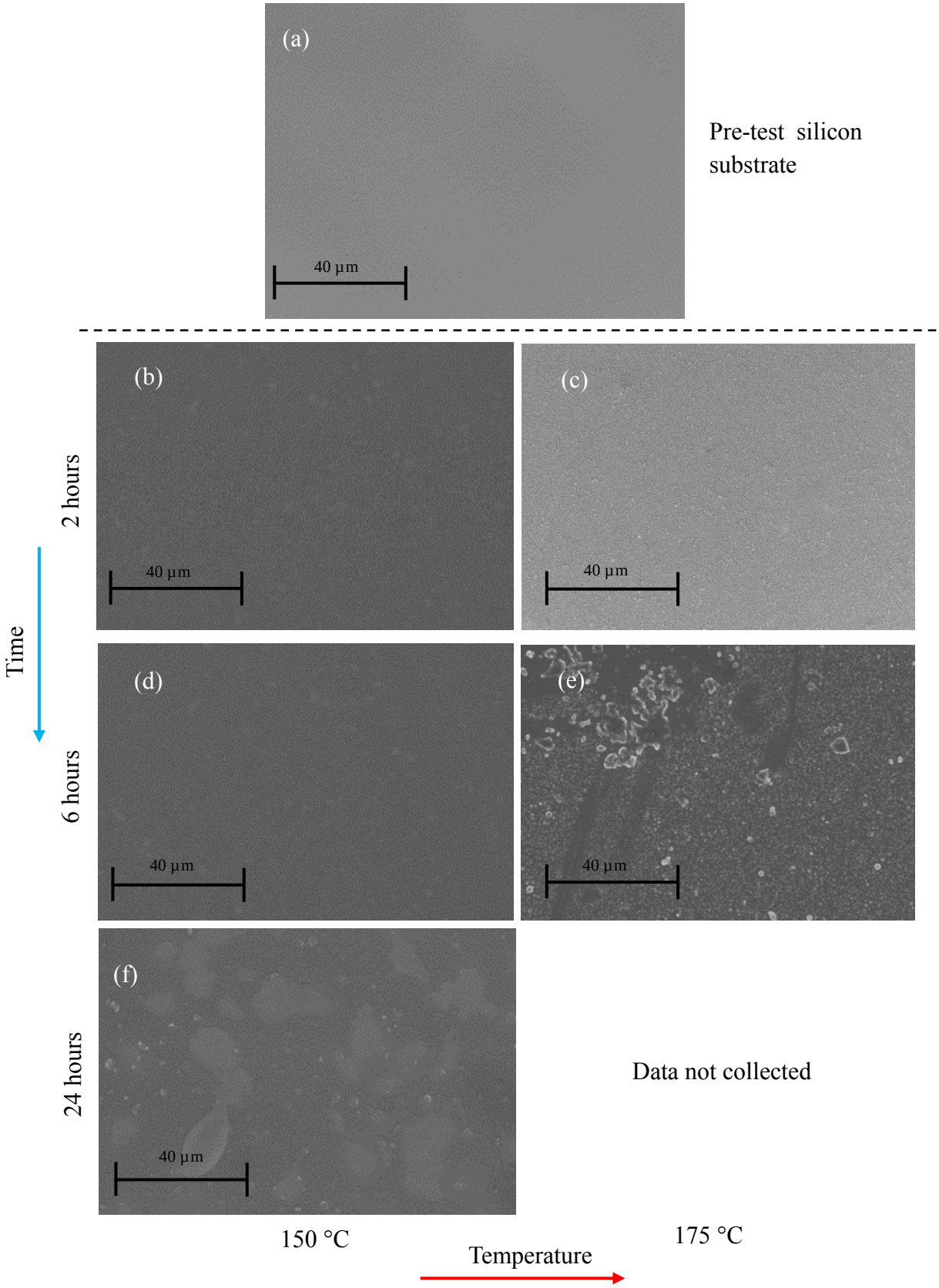

Fig. 9: Surface morphology of (a) Si substrate before test; (b) Si in PP 150 ºC 2h; (c) Si in PP 175 ºC 2h; (d) Si in PP 150 ºC 6h (e) Si in PPIL 175 ºC 6h and (f) Si in PPIL 150 ºC 24h.

It is clear that PP creates a thermal film. The SEM results confirm that a few changes occur in the surface morphology, especially, when the temperature is increased to 175 ^{o}C.

EDS results showed that the presence of oxygen and carbon is significantly increased in the silicon surface after the generation of the PP thermal film. However, phosphorus still could not be detected and a more surface sensitive technique is employed to confirm the formation of the PP thermal film.

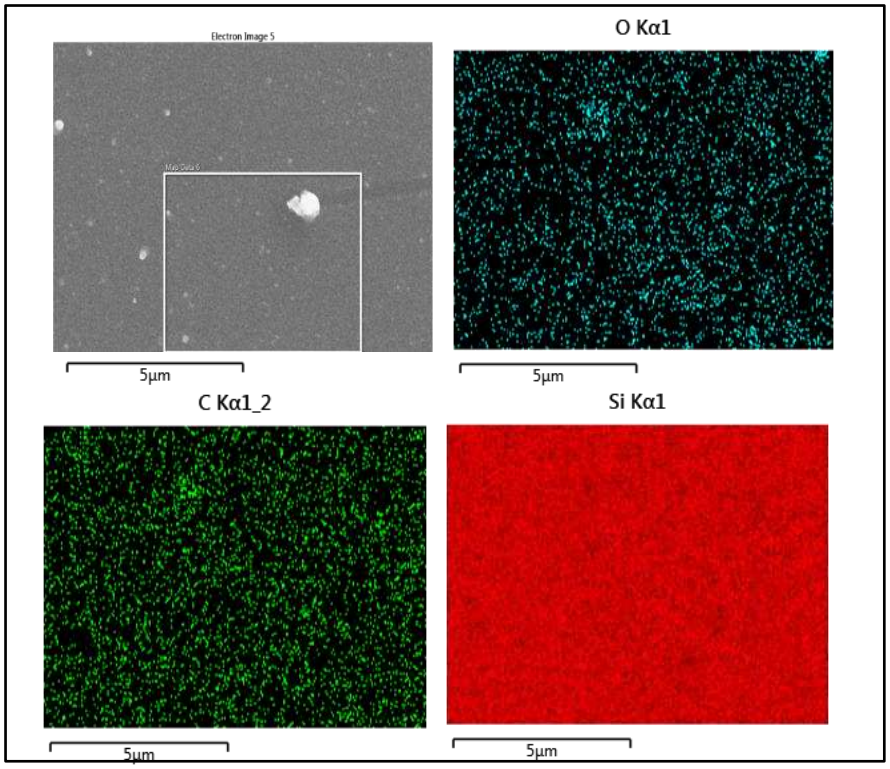

Fig. 10: The EDS map of PP thermal film at 150 ^{o}C and for 24 h.

XPS results demonstrate that there is a thermal film presents at the lowest applied temperature with the lowest period; 150 ^{o}C and 2h. The film is detected by comparing P2s peak (Figure 11) with silicon substrate before the formation of thermal film. Again, as observed in the ZDDP thermal film, phosphorus element and Si2s related peaks are diminished compared with the P2s peak for silicon before the formation of thermal film.

Two peaks are obtained at 150 ^{o}C, 2h with their binding energies are 188.6 eV and 191.5 eV respectively. The former can be assigned to phosphate comparable to a ZDDP thermal film. The second peak at 191.5 eV is assigned to P-O-Si (41). Only one peak at 191.5 eV is obtained in the second examined condition, 175 ^{o}C and 6h which means that P-O-Si solely exists at this condition.

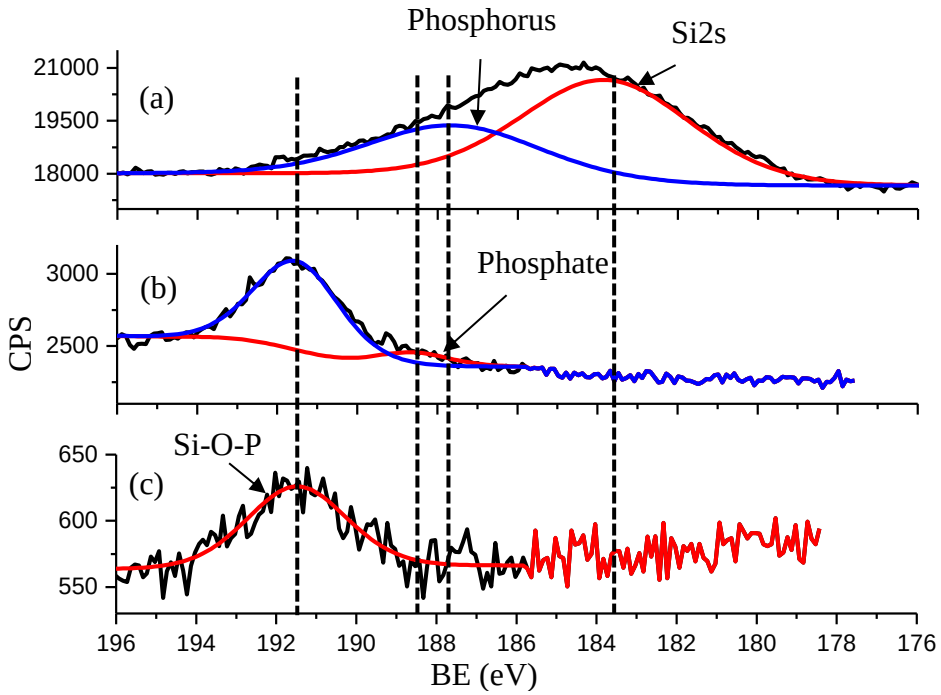

Fig. 11**:** P2s peak for (a) silicon before experiment, (b) PP thermal film formed at 2h and 150 ^{o}C and (c) PP thermal film formed at 6h and 175 ^{o}C

Lastly, table 3-2 presents the chemical composition of PP thermal film at two conditions (150 ^{o}C for 2 hours and 175 ^{o}C for 6 hours). The results show a plenty of carbon exists which can be resulted from the traces of both the base lubricant (PAO) and PP. The atomic percentage of phosphorus increases with the increase of time and temperature. This finding is in agreement SEM results since the morphology of the PP thermal film suggests that the increase of time/temperature increases film thickness.

4. Discussion

4.1 Film formation mechanism

The ZDDP thermal film formation mechanism seems to follow the same mechanism as presented in (49) for a steel surface. Consequently, at 150°C for 2h; three layers are formed which are ZnS (Figs. 6b and Figs. 7a), phosphate (Fig. 8b) and P-O-Si layers (Fig. 8b).

The increase of time and temperature to 175°C for 6h shows that ZnS layer is replaced by ZnO as the sulfur peak is diminished as depicted in Fig. 6c and the Zn2p peak is shifted by 0.6 eV (Fig. 7b). This finding is confirmed when 6 spots are scanned by XPS for two silicon samples in the same conditions (175°C for 6h). Further, the increase in time and temperature leads to an increase in the ratio of Si-O-P to phosphate which suggests the phosphate transformed to Si-O-P.

The ability of ILs to be decomposed at temperature by far lower than their decomposition temperature as stated in (50) and the presence of P-O-Si suggest that a chemical reaction occurs between PP and silicon surface. The formation mechanism of PP thermal film is summarized in Fig. 12. The reaction between PP and silicon surface at 150°C for 2h results in the formation of phosphate and P-O-Si layers within the bulk of the thermal film (Fig. 11b). The increase of time and temperature to 175°C and 6h seems to create a single layer thermal film consisting of P-O-Si as presented in Fig. 11c. This finding suggests that the phosphate layer is transforming to P-O-Si with the increase of time and temperature.

Despite the differences between the components of ZDDP and PP thermal films; both resulting phosphorus species being bond to the silicon surface as shown in Fig. 8 and Fig.11.

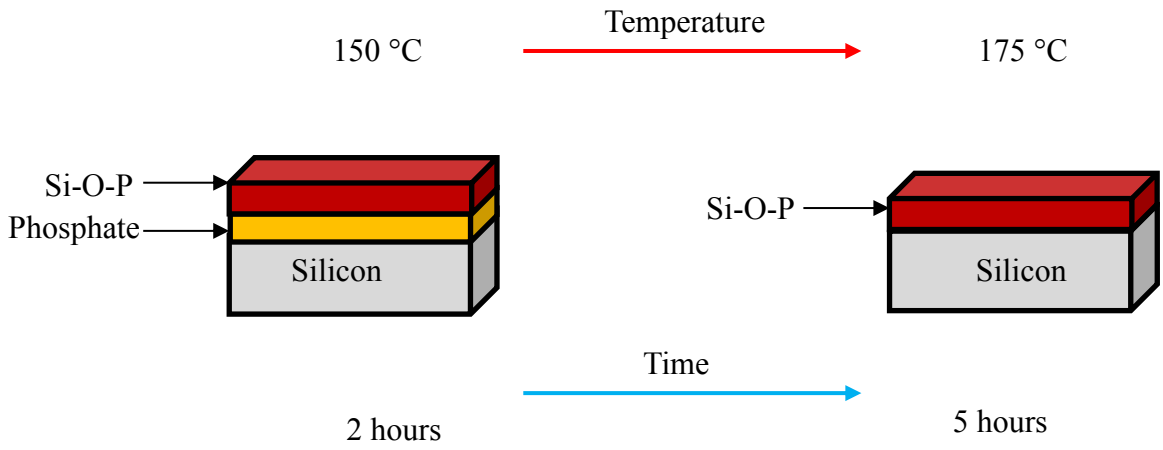

Fig.12: PP thermal film formation mechanism.

4.1 Film thickness

Phosphonium phosphate thermal film remains undetectable by ATR-FTIR and EDS even at the longest time 24hrs and 150^{o}C. However, XPS results confirm the formation of a thermal film even at the shortest time of 2h and the lowest temperature of 150^{o}C. In contrast, ZDDP thermal film is detected by EDS and FTIR in three different conditions; 150 ^{o}C 24h, 175 ^{o}C 2h and 175 ^{o}C 6h (see Fig. 3). Therefore, it is clearly seen from the results that ZDDP thermal films are thicker than PP thermal films. The lower decomposition temperature of ZDDP additives compared to PP (51) can lead to a higher adsorption of ZDDP molecules to react with the silicon substrate which leads to form thicker films.

Formation of a thin thermal film by PP can also be related to the absence of metal cation, such as Zn^{2+} in ZDDP, to feed the chemical reaction. This means that the chemical reaction is not sustainable and PP reacts with silicon when they are in direct contact. To check the validity of this assumption, the time is increased into 24 hours but the film is still not thick enough to be detected by either ATR-FTIR or EDS. This finding is in agreement with the recent finding by Zhou at al (52) when the formation mechanism of PP tribofilm is studied and it is found that PP tribofilm formation is unsustainable unless a positive cation is provided from wear debris. This is examined in our tribological work that will be published in due course.

5. Conclusion

A comparative study is done to investigate the reactivity of oil-soluble IL and ZDDP with a silicon surface at elevated temperatures and the following conclusions can be drawn:

- Both additives react with the silicon surface and form thermal films.
- The increase of time and temperature results in the increase of the thermal film thickness and film homogeneity.
- ZDDP forms thicker thermal film than PP in the same conditions.
- The formation pathways of phosphorus in both additives are comparable.
- Both additives form P-O-Si as a result of the chemical reaction between phosphorus and silicon surface.
- The above findings can confirm that, in contrast to ZDDP, the formation of PP thermal film is not sustainable due to the absence of a positive ion that can feed the reaction to sustain it.

Acknowledgement:

This project is funded by the University of Leeds, LARS fellowship. The authors would like to thank Dr. Filippo Mangolini for his help in this work.

6. References

1. Holmberg K, Andersson P, Nylund N-O, Mäkelä K, Erdemir A. Global energy consumption due to friction in trucks and buses. Tribology International. 2014;78:94-114.

2. Holmberg K, Andersson P, Erdemir A. Global energy consumption due to friction in passenger cars. Tribology International. 2012;47:221-34.

3. Minami I. Ionic liquids in tribology. Molecules. 2009;14(6):2286-305.

4. Somers AE, Howlett PC, MacFarlane DR, Forsyth M. A review of ionic liquid lubricants. Lubricants. 2013;1(1):3-21.

5. Palacio M, Bhushan B. A review of ionic liquids for green molecular lubrication in nanotechnology. Tribology Letters. 2010;40(2):247-68.

6. Zhou Y, Qu J. Ionic Liquids as Lubricant Additives – a Review. ACS Applied Materials & Interfaces. 2016.

7. Qu J, Luo H, Chi M, Ma C, Blau PJ, Dai S, et al. Comparison of an oil-miscible ionic liquid and ZDDP as a lubricant anti-wear additive. Tribology International. 2014;71:88-97.

8. Erdemir A, Eryilmaz O. Achieving superlubricity in DLC films by controlling bulk, surface, and tribochemistry. Friction. 2014;2(2):140-55.

9. Ala'A A-A, Eryilmaz O, Erdemir A, Kim SH. Nano-texture for a wear-resistant and near-frictionless diamond-like carbon. Carbon. 2014;73:403-12.

10. Rudnick LR. Lubricant additives: chemistry and applications: CRC press; 2009.

11. Spikes H. The history and mechanisms of ZDDP. Tribology letters. 2004;17(3):469-89.

12. Nicholls MA, Do T, Norton PR, Kasrai M, Bancroft GM. Review of the lubrication of metallic surfaces by zinc dialkyl-dithiophosphates. Tribology International. 2005;38(1):15-39.

13. Mangolini F, Rossi A, Spencer ND. Influence of metallic and oxidized iron/steel on the reactivity of triphenyl phosphorothionate in oil solution. Tribology International. 2011;44(6):670-83.

14. Zhang Z, Yamaguchi E, Kasrai M, Bancroft G. Tribofilms generated from ZDDP and DDP on steel surfaces: Part 1, growth, wear and morphology. Tribology Letters. 2005;19(3):211-20.

15. Li H, Somers AE, Rutland MW, Howlett PC, Atkin R. Combined Nano-and Macrotribology Studies of Titania Lubrication Using the Oil-Ionic Liquid Mixtures. ACS Sustainable Chemistry & Engineering. 2016;4(9):5005-12.

16. Yu B, Bansal DG, Qu J, Sun X, Luo H, Dai S, et al. Oil-miscible and non-corrosive phosphonium-based ionic liquids as candidate lubricant additives. Wear. 2012;289:58-64.

17. Qu J, Bansal DG, Yu B, Howe JY, Luo H, Dai S, et al. Antiwear performance and mechanism of an oil-miscible ionic liquid as a lubricant additive. ACS applied materials & interfaces. 2012;4(2):997-1002.

18. Zhou Y, Leonard DN, Guo W, Qu J. Understanding Tribofilm Formation Mechanisms in Ionic Liquid Lubrication. Scientific Reports. 2017;7.

19. Huang G, Yu Q, Ma Z, Cai M, Zhou F, Liu W. Oil-soluble ionic liquids as antiwear and extreme pressure additives in poly-α-olefin for steel/steel contacts. Friction. 2017:1-14.

20. Qu J, Barnhill WC, Luo H, Meyer HM, Leonard DN, Landauer AK, et al. Synergistic Effects Between Phosphonium-Alkylphosphate Ionic Liquids and Zinc Dialkyldithiophosphate (ZDDP) as Lubricant Additives. Advanced Materials. 2015;27(32):4767-74.

21. T.F.J. Quinn JLSaDMR, New Developments in the Oxidational Theory of the Mild Wear of Steels, Proc. Int. Conf. on Wear of Materials, Dearborn, Michigan, 16-18 April 1979, editors K.C. Ludema, W.A. Glaeser and S.K. Rhee, Publ. American Society of Mechanical Engineers, New York, 1979, pp. 1-11.

22. Parsaeian P, Ghanbarzadeh A, Van Eijk MC, Nedelcu I, Neville A, Morina A. A new insight into the interfacial mechanisms of the tribofilm formed by zinc dialkyl dithiophosphate. Applied Surface Science. 2017;403:472-86.

23. Dorgham A, Parsaeian P, Neville A, Ignatyev K, Mosselmans F, Masuko M, et al. In situ synchrotron XAS study of the decomposition kinetics of ZDDP triboreactive interfaces. RSC Advances. 2018;8(59):34168-81.

24. Dorgham A, Parsaeian P, Azam A, Wang C, Morina A, Neville A. Single-asperity study of the reaction kinetics of P-based triboreactive films. Tribology International. 2018.

25. Akbari S, Kovač J, Kalin M. Effect of ZDDP concentration on the thermal film formation on steel, hydrogenated non-doped and Si-doped DLC. Applied Surface Science. 2016;383:191-9.

26. Fuller MLS, Kasrai M, Bancroft GM, Fyfe K, Tan KH. Solution decomposition of zinc dialkyl dithiophosphate and its effect on antiwear and thermal film formation studied by X-ray absorption spectroscopy. Tribology international. 1998;31(10):627-44.

27. Li Y-R, Pereira G, Lachenwitzer A, Kasrai M, Norton PR. Studies on ZDDP thermal film formation by XANES spectroscopy, atomic force microscopy, FIB/SEM and 31P NMR. Tribology Letters. 2008;29(1):11-22.

28. Jones R, Coy R. The chemistry of the thermal degradation of zinc dialkyldithiophosphate additives. Asle Transactions. 1981;24(1):91-7.

29. Coy R, Jones R. The thermal degradation and EP performance of zinc dialkyldithiophosphate additives in white oil. ASLE transactions. 1981;24(1):77-90.

30. Aktary M, McDermott MT, McAlpine GA. Morphology and nanomechanical properties of ZDDP antiwear films as a function of tribological contact time. Tribology letters. 2002;12(3):155-62.

31. Crobu M, Rossi A, Mangolini F, Spencer ND. Tribochemistry of bulk zinc metaphosphate glasses. Tribology letters. 2010;39(2):121-34.

32. Crobu M, Rossi A, Spencer ND. Effect of chain-length and countersurface on the tribochemistry of bulk zinc polyphosphate glasses. Tribology letters. 2012;48(3):393-406.

33. Burkinshaw M, Neville A, Morina A, Sutton M. Calcium sulphonate and its interactions with ZDDP on both aluminium–silicon and model silicon surfaces. Tribology International. 2012;46(1):41-51.

34. Jimenez A, Morina A, Neville A, Bermudez M. Surface interactions and tribochemistry in boundary lubrication of hypereutectic aluminium—silicon alloys. Proceedings of the Institution of Mechanical Engineers, Part J: Journal of Engineering Tribology. 2009;223(3):593-601.

35. Landauer AK, Barnhill WC, Qu J. Correlating mechanical properties and anti-wear performance of tribofilms formed by ionic liquids, ZDDP and their combinations. Wear. 2016;354:78-82.

36. Bruker. Attenuated Total Reflection (ATR) – a versatile tool for FT-IR spectroscopy In: Optics B, editor.: Bruker Optics BOPT-4000352-01; 2011.

37. Socrates G. Infrared and Raman characteristic group frequencies: tables and charts: John Wiley & Sons; 2004.

38. Wassilkowska A, Czaplicka-Kotas A, Bielski A, Zielina M. An analysis of the elemental composition of micro-samples using EDS technique. Czasopismo Techniczne. 2015;2014(Chemia Zeszyt 1-Ch (18) 2014):133-48.

39. Mukhopadhyay SM. Sample preparation for microscopic and spectroscopic characterization of solid surfaces and films. Sample Preparation Techniques in Analytical Chemistry. 2003;162(9):377-411.

40. Watts JF, Wolstenholme J. An introduction to surface analysis by XPS and AES. An Introduction to Surface Analysis by XPS and AES, by John F Watts, John Wolstenholme, pp 224 ISBN 0-470-84713-1 Wiley-VCH, May 2003. 2003:224.

41. Gouzman I, Dubey M, Carolus MD, Schwartz J, Bernasek SL. Monolayer vs. multilayer self-assembled alkylphosphonate films: X-ray photoelectron spectroscopy studies. Surface Science. 2006;600(4):773-81.

42. Mangolini F, Rossi A, Spencer ND. Chemical reactivity of triphenyl phosphorothionate (TPPT) with iron: an ATR/FT-IR and XPS investigation. The Journal of Physical Chemistry C. 2010;115(4):1339-54.

43. Scofield J. Hartree-Slater subshell photoionization cross-sections at 1254 and 1487 eV. Journal of Electron Spectroscopy and Related Phenomena. 1976;8(2):129-37.

44. Tanuma S, Powell C, Penn D. Calculations of electron inelastic mean free paths. Surface and Interface Analysis. 2005;37(1):1-14.

45. Reilman RF, Msezane A, Manson ST. Relative intensities in photoelectron spectroscopy of atoms and molecules. Journal of Electron Spectroscopy and Related Phenomena. 1976;8(5):389-94.

46. Crobu M, Rossi A, Mangolini F, Spencer ND. Chain-length-identification strategy in zinc polyphosphate glasses by means of XPS and ToF-SIMS. Analytical and bioanalytical chemistry. 2012;403(5):1415-32.

47. Langer D, Vesely C. Electronic core levels of zinc chalcogenides. Physical Review B. 1970;2(12):4885.

48. Gaarenstroom S, Winograd N. Initial and final state effects in the ESCA spectra of cadmium and silver oxides. The Journal of Chemical Physics. 1977;67(8):3500-6.

49. Johnson D, Hils J. Phosphate Esters, Thiophosphate Esters and Metal Thiophosphates as Lubricant Additives. Lubricants. 2013;1(4):132.

50. Maton C, De Vos N, Stevens CV. Ionic liquid thermal stabilities: decomposition mechanisms and analysis tools. Chemical Society Reviews. 2013;42(13):5963-77.

51. Improving Wind Turbine Gearbox Reliability WM, S. Butterfield, B. McNiff, NREL/CP-500-41548, European Wind Energy Conference, Milan, Italy, May 2007.

52. Zhou Y, Leonard DN, Guo W, Qu J. Understanding Tribofilm Formation Mechanisms in Ionic Liquid Lubrication. Scientific reports. 2017;7(1):8426.

Table 3-1: XPS results of the chemical composition of ZDDP thermal films.

Condition	C at%	O at%	Si at%	S at%	Zn at%	P at%
150 ^{o}C and 2 hours	88.30	3.90	7.4	0.09	0.08	0.23
175 ^{o}C and 6 hours	88.9	8.1	0.36	0.0	0.08	2.56

Table 3-2: XPS results of the chemical composition of PP thermal film.

Condition	C %	O %	Si%	S%	Zn %	P %
150 ^{o}C and 2 hours	91.0	5.2	3.6	0.0	0.0	0.2
175 ^{o}C and 6 hours	91.0	4.7	3.4	0.0	0.0	0.9